International Journal of Structural Integrity

Flexural Capacity of Bi-Directional GFRP Strengthened RC Beams with end Anchorages: Experimental and Theoretical Studies

Journal:	*International Journal of Structural Integrity*
Manuscript ID	IJSI-04-2018-0021
Manuscript Type:	Research Paper
Keywords:	Anchorage systems, Bi-directional glass fibre Reinforced polymer, Ductility, Ultimate moment capacity, Deflection and flexural effectiveness

Flexural Capacity of Bi-Directional GFRP Strengthened RC Beams with end Anchorages: Experimental and Theoretical Studies

ABSTRACT

This paper presents the results of experimental and theoretical studies on the flexural capacity of reinforced concrete (RC) beams strengthened using externally bonded bi-directional glass fibre reinforced polymer (GFRP) composites and different end anchorage systems. A series of nine RC beams with a length of 1600mm and a cross-section of 200mm depth and 100mm width were prepared and externally strengthened in flexure with bi-directional GFRP composites. These strengthened beams were anchored with three different end anchorage systems namely closed GFRP wraps, GFRP U-wraps, and mechanical anchors. All these beams were tested with four-point bending system up to failure. The obtained experimental results demonstrate a significant increase in the flexural performance of the GFRP strengthened beams with regard to the ultimate load carrying capacity and stiffness. The experimental results also show that GFRP strengthened beams with no end anchorages experienced intermediate concrete (IC) debonding failure at the GFRP plate end, whereas, all the GFRP Strengthened beams with different end anchorage systems failed in rupture of GFRP with concrete crushing. The theoretical results revealed no significant difference among the relevant design guidelines with regard to the predicted ultimate moment capacities of the bi-directional GFRP strengthened RC beams. However, the results show that ACI Committee 440 (2008) design recommendation provides reasonably acceptable predictions for the ultimate moment capacities of the tested beams strengthened externally with bi-directional GFRP reinforcement followed by FIB Bulletin 14 (2001) and eventually JSCE (1997).

Keywords: Anchorage systems, Bi-directional glass fibre Reinforced polymer, Deflection and flexural effectiveness, Ductility, Ultimate moment capacity.

1. INTRODUCTION

A significant number of reinforced concrete (RC) structures are required to be retrofitted due to one or combination of several factors including constructions faults, original design limits, alterations in usage, excessive loading, and natural disasters or aggressive environmental conditions. The conventional strengthening techniques such as external steel plate bonding method, section enlargement, and external post-tensioning system have been used to extend service life and retrofit the damaged reinforced concrete structures. However, in recent decades, the application of externally bonded fibre reinforced polymer reinforcement has been an extensively used technique for retrofitting the damaged reinforced concrete structures due to its potential advantageous characteristics that include high strength-to-weight ratio, high stiffness and ease of installation without any external supports (Hollaway 2010; Teng et al. 2002).

Substantial experimental investigations (Anania et al., 2005; Benjeddou et al., 2007; Carlos et al., 2018; Ceroni, 2010; Gao et al., 2005; Hosen et al., 2018; Jayaprakash et al., 2015; Kim and Shin, 2011; Li et al., 2008; Nurbaiah et al., 2010; Rafi et al., 2008; Spadea et al., 2015; Sundarraja and Rajamohan, 2008; Toutanji et al., 2006; Triantafyllou et al., 2017; Yang et al., 2018) have been conducted on the flexural strengthening of RC beams using fibre reinforced polymer composites. These studies have proved that external FRP reinforcement is effective in enhancing the flexural performance of the strengthened RC beams with regards to ultimate strength and stiffness. However the strengthened beams have encountered different modes of failure that include FRP rupture, crushing of concrete, shear failure, critical diagonal crack debonding, concrete cover separation failure, plate end interfacial debonding and intermediate crack-induced interfacial debonding (IC) (J.G. Teng 2001; Leung and Yang 2006; Wang and Zhang 2008; Teng et al. 2003; Teng and Chen 2007; Hollaway, L.C. and Teng 2008). It has been noted by researchers (Aram et al., 2008; Bencardino et al., 2002; Chahrour and Soudki, 2005; Fu et al., 2018; Said and Wu, 2008) that reinforced concrete beams strengthened externally with FRP experienced premature debonding failure of FRP reinforcement from the concrete surface. However, this premature debonding failure mode limits the strengthening capacity of the FRP composites.

The effect of U-Jacket anchors on strengthening and ductility as well as on the general performance of externally reinforced beams was first discussed and clarified in Spadea et al. (1998) and Spadea et al. (2000). Recently, Pham and Al-Mahaidi (2006) investigated the behaviour and flexural performance of 260mm x140mm RC beams retrofitted with CFRP composites. The CFRP strengthened beams were anchored with unidirectional CFRP U-straps of 209GPa modulus of elasticity at the CFRP plate ends or at 180mm spacing along the shear span. The study showed that addition of U-Jacket anchors at the FRP plate end significantly enhanced the efficiency of FRP system by preventing intermediate span and end debonding failures. The result also indicates an excellent performance of the U-Jacket anchors when applied at a certain spacing to the shear span of retrofitted RC beams, as the mechanism of IC debonding failure was prevented or delayed. Subsequently, Al-Amery and Al-Mahaidi (2006) studied the coupling shear-flexural retrofitting of RC beams with CFRP U-jackets placed at 200mm spacing along the span of the beams and tested in four and three-point bending system. The results have shown that the presence of CFRP U-straps spaced at 200mm along the span of the beam significantly prevented the debonding of CFRP sheet and it limits the interfacial slip between CFRP in the beam soffit and the concrete section up to 10%. It was also found that using CFRP U-straps to anchor the flexural CFRP sheets could substantially enhance the flexural strength to 95% in addition to increased ductility.

Duthinh and Starnes (2001) studied the flexural effectiveness of reinforced concrete beams strengthened in flexure with CFRP of 50mm width, the thickness of 1.2 mm and elastic modulus of

155GPa. Out of seven specimens, three were anchored with mechanically fastened steel plates of 203mm width over the FRP plate ends. A clamping force of 15-25kN was then applied to two bolts which are torqued to 0.4kNm. The experimental results have shown that the combination of adhesion and clamping could enhance the FRP anchorage capacity as expected because both diagonal and transverse wraps anchored the flexural CFRP to a strain increase of 58% and 43% of the rupture strain. The result also demonstrated that the improved ultimate strain of the anchored plates was up to 1.14%, (i.e.) 60% of the rupture strain, as a result of adhesion and clamping. However, the authors also concluded that the mechanism of failure was debonding of CFRP laminate usually initiating from diagonal or transverse shear cracking zone.

A new hybrid system comprising mechanically fastened (MF-FRP) system and common externally bonded (EB-FRP) systems was investigated by Wu and Huang (2008). The experimental program consisted of beam specimens strengthened with 2, 4 and 6 layers of CFRP strips. The hybrid system failed by two apparent failure patterns namely, the CFRP rupture at mid-span in beams strengthened with 2 and 4 layers FRP strips, and the total debonding of CFRP strips which occurred in beams strengthened with 6 layers of CFRP strips. The results showed that beams mechanically fastened with 4 and 6 layers of FRP sheets exhibits higher flexural strength than the beams strengthened with 2 layers of CFRP and no fasteners. The authors further concluded that the use of hybrid plate bonding system could significantly improve the flexural capacity and bond strength in addition to the moment of resistance enhancement.

In recent decades, different anchorage systems including U-jacket anchors, mechanically fastened metallic anchors, and FRP anchors in order to enhance the efficiency and to prevent the premature debonding of FRP reinforcement have investigated (Chahrour and Soudki 2005; Leung 2002; Smith 2010; L. Lam and J.G. Teng 2001; Zhang and Smith 2012; Yalim et al. 2008; Smith and Teng 2003; Buyle-Bodin and David 2004). It has been proved that the anchoring systems could enhance the load carrying capacity and ductility of RC beams strengthened with FRP composites. Moreover, it was found that the end anchorages could provide an efficient load transfer between concrete and the bonded FRP reinforcement in addition to FRP strain level enhancement prior to failure (Grelle and Sneed 2013; Kalfat and Smith 2013; Baggio et al. 2014). In due course, the literature review reveals that the number of experimental results of beams with anchorages are not extensively investigated and validated with the different existing codes including ACI Committee 440 Report (2008), Fédération Internationale Du Béton (FIB Bulletin 14) (2001) and Japan Society of Civil Engineers (JSCE) (1997). Reinforced concrete beams strengthened in flexure with bi-directional GFRP composites and plate end anchorages are considered and reported in this study. The end anchored flexural bi-directional GFRP sheets are placed at 150mm away from the beam supports in order to avert end-of-plate failure.

In This paper, the influence of the number of bi-directional GFRP layers and different end anchorages on flexural capacity of strengthened reinforced concrete (RC) beams is investigated. The investigation covers two parts. The first part includes a detailed experimental investigation to study the influence of different end anchorage systems on the ultimate load carrying capacity and failure mechanism of RC beams strengthened externally with bi-directional GFRP reinforcement. A comparison of experimental and theoretical results using three different design guidelines predictions (i.e. ACI Committee 440 Report, (2008); Japan Society of Civil Engineers, (JSCE), (1997); and Fédération Internationale Du Béton (FIB Bulletin 14), (2001)) is presented in the second part of the research study.

2. EXPERIMENTAL INVESTIGATION

2.1 Preparation of RC Beams and Material Properties reluctant

A total of nine reinforced concrete beams were cast in concrete mixing laboratory with a targeted concrete grade of 20N/mm^2. All these beams were of 1600mm span length and a cross-section dimension of 100mm×200mm. All these beams were designed to fail in flexure using Eurocode 2: design guideline for concrete structures (BS EN 1992-1-1E, 2004). These beams were reinforced with a longitudinal compression reinforcement of 2-10mm in diameter and tensile reinforcement of 2-12mm in diameter. The beams were firmly reinforced in the shear zones to prevent shear failure. The steel stirrups at shear and flexural zones were placed with 6mm diameter at 50mm and 100mm centre to centre, respectively.

2.1.1 Concrete

The concrete mix was prepared in accordance with BS 1881 part 125 (1986) design guidelines, in order to achieve the targeted compressive strength of 20N/mm^2 at 28 days. The mix proportion by weight of cement: fine aggregate: coarse aggregate: water was 1:1.38:2.42:0.50, respectively. Ordinary Portland Cement, sand, crushed coarse aggregates of 20mm maximum size, and potable water was used to prepare the concrete mix at Concrete Mixing Laboratory, University of Nottingham, Malaysia Campus. A total of nine beams were cast with four different batches of concrete and were cured for 28 days before testing. Four concrete cube specimens of 100mm×100mm×100mm size were also prepared for each batch to determine the compressive strength of concrete cube at the age of 28 days. The results of compressive strength of concrete cubes are presented in Table-1.

2.1.2 Steel reinforcement

The average tensile strength of 12mm and 10mm steel rebar were of 460.5N/mm^2 and 251.82N/mm^2, respectively. Figure-1 portrays the reinforcement details of the RC beams.

2.1.3 FRP Composites

All the beams were reinforced externally with bi-directional GFRP reinforcement with two-component epoxy resin. As recommended in the manufacturer's manual, the bi-directional GFRP sheet was applied using manual wet layup technique with a resin and hardener mix ratio of 1:2. The material properties of bi-directional GFRP reinforcement and epoxy resin are presented in Table-2.

2.2 Specimen Description

The first specimen was retained as control beam with no external bi-directional GFRP reinforcement which is labelled as CB, and the remaining eight specimens were divided into four series. Two beams, within each series, were bonded externally with 1 and 2 layers of bi-directional GFRP reinforcement along the soffit of the beams. The specimens in first (i.e. FSB-CA1 and FSB-CA2) and second (i.e. FSB-UA1 and FSB-UA2) series used closed and U-wrap anchorages with 2 layers of bi-directional GFRP (i.e. 100 mm width) strip bands at the ends of flexural reinforcement, respectively. The third series, labelled as FSB-SA1 and FSB-SA2, were anchored with 100mm x 100mm x 2mm steel plate at the ends of GFRP reinforcement and the specimens in the fourth series with 1 and 2 layers of flexural bi-directional GFRP reinforcement were designated as FSB-C1 and FSB-C2 with no plate end anchor, respectively. The outline of the test beams is presented in Table-3 and illustrated in Figures-2(a) through (e).

2.3 Test Procedure

A schematic diagram of the experimental set-up of the reinforced concrete beam is shown in Figure-3. All the beam specimens were subjected to four-point bending test. Prior to testing, the beam specimens were painted white for ease of identification of cracks. A 30 tonnes capacity testing frame was used to perform the four-point bending test. The load was applied using the hydraulic jack at equal interval until failure. The dial gauge was placed at the centre of the beam to measure the mid-span deflection. The crack patterns of the beam specimens at different stages of loading were observed.

3. RESULTS AND DISCUSSION

3.1 Load Deflection Curve

Control Beam (CB): The applied load-deflection behaviour of the control beam is illustrated in Figure-4. The curve shows a tri-linear response which is typical behaviour of reinforced concrete beams with no external GFRP reinforcement. Upon loading, the early stage of the deflection curve shows a region with relatively high stiffness prior to the formation of flexural cracks. The flexural cracks, in the bending zone, occurred at an applied load of 22.5kN, however, at later stages, the stiffness of the deflection curve decreases as the concrete cracks and this region exhibits the post-cracking behaviour of the beam. The stiffness of the curve continues to decrease with an increase in the applied load up to yielding of steel reinforcement. At last, the beam failed in flexure due to the yielding of steel reinforcement at a peak load of 101.05kN and a maximum deflection of 44.81mm. Moreover, the beam achieved a ductile behaviour beyond yield point up to the failure load. Figure-5 shows the flexural failure pattern of control beam.

First Series: The first series consisted of two beams (i.e. FSB-CA1 and FSB-CA2) strengthened externally with 1, and 2 layers of bi-directional GFRP reinforcement and these beams were anchored with two layers of closed GFRP strips with a width of 100mm. The applied load-deflection behaviour of the control and strengthened beams is shown in Figure-6. The ductility of bi-directional GFRP strengthened beams with closed GFRP anchorage strips was relatively less as compared to the control beam CB. These specimens FSB-CA1 and FSB-CA2 exhibited similar stiffness trend before yielding of steel reinforcement despite the fact that the beams were bonded with different GFRP layers and identical anchoring system. From Figure-6, it should be noted that the loss of ductility of the beam FSB-CA2 is relevant compared both with that of the control beam and with the beam FSB-CA1. This result shows that the stiffness of GFRP strengthened beam could be increased by increasing the thickness of GFRP reinforcement. However, it might not increase the ductility of the beam. Moreover, the beam FSB-CA2 with two layers of GFRP reinforcement attained better performance in terms of flexural capacity as compared to the beam FSB-CA1 with one layer of GFRP reinforcement. The flexural cracks in these GFRP strengthened beams were observed at a load of 42.1kN. These beams FSB-CA1 and FSB-CA2 were failed in flexure with rupture of GFRP reinforcement and followed by crushing of concrete at a peak load of 146.4kN and 170.18kN, respectively. The maximum deflection at failure for FSB-CA1 and FSB-CA2 was 24.50mm and 26.97mm, respectively. No debonding failure was observed in the Anchorage region of the tested beams. Figure-7 portrays the failure pattern of bi-directional GFRP strengthened beams FSB-CA1 and FSB-CA2.

Second Series: Beams in the second series, designated as FSB-UA1 and FSB-UA2 (i.e. bonded with 1 and 2 layers of GFRP reinforcement), were anchored with two layers of bi-directional GFRP U-strips of 100mm width. The load-deflection curve for FSB-UA1, FSB-UA2, and CB beams is shown in Figure-8. As seen in the first series beams, the deflection curve of beams FSB-UA1 and FSB-UA2 experienced less ductile behaviour as compared to the control beam CB. It also demonstrated a tri-linear response (i.e. bounded by three different stages). The first stage is the region with higher stiffness before first cracking occurs; the second part is the post-cracking stage after the formation of crack with a decrease in flexural stiffness; the third stage represents a region where a loss in stiffness occurred after the yielding of internal steel reinforcement up to failure. The deflection curves of beams FSB-UA1 and FSB-UA2 experienced similar stiffness trend till the steel yielding stage. However, prior to failure, higher performance in flexural stiffness was observed in the FSB-UA2 beam as compared to the beam FSB-UA1 which was due to the effect of the number of GFRP layers. The flexural cracks in both FSB-UA1 and FSB-UA2 occurred at the constant bending zone of the beam. Upon loading, the flexural cracks of these beams occurred at a load of 42.1kN. Failure of FSB-UA1 and FSB-UA2 beams occurred when the bi-directional GFRP reinforcement ruptured in the constant moment region of the beams at a peak load of 145.45kN and 155.35kN, with the corresponding maximum deflection of 26.44mm and 24.98mm, respectively. Similar to beams in the first series with closed GFRP anchorages, no debonding failure was observed at the anchorage zones of the beams in the second series. The failure pattern of beams FSB-UA1 and FSB-UA2 is shown in Figure-9

Third Series: The third series comprised of two beams designated as FSB-SA1 and FSB-SA2 strengthened in flexure with 1 and 2 layers of GFRP reinforcement and anchored with 100mm x 100mm x 2mm steel plate at the ends of flexural GFRP reinforcement. Figure-10 portrays the load-deflection behaviour of the GFRP strengthened (i.e. third series) and control beams. The curves for both FSB-SA1 and FSB-SA2 also exhibited tri-linear behaviour as seen in the first and second series beams. However, as compared to the control beam, these beams also experienced less ductile behaviour. From Figure-10, it evident that the beam FSB-SA2 with two layers of GFRP reinforcement exhibited better performance in terms of flexural stiffness over the beam FSB-SA1 having one layer of GFRP reinforcement. Flexural cracks began to occur at a load of 33.7kN and 42.1kN for FSB-SA1 and FSB-SA2 beams, respectively. The beams were failed in GFRP rupture at the constant moment region as the applied load attained a peak value of 143.55kN and 156.90kN with the corresponding maximum deflection values of 26.92 mm and 23.88 mm for the beams FSB-SA1 and FSB-SA2, respectively. However, no failure was observed in the region of steel plate anchors in both the specimens in the third series. The typical modes of failure of beams in the third series are shown in Figure-11.

Fourth Series: The fourth series beams, designated as FSB-C1 and FSB-C2, were strengthened with 1 and 2 layers of GFRP along the soffit surface with no anchorages. The beams in this series are considered as control beams for the first, second, and the third series beams to evaluate the effect of different anchorage systems on the GFRP strengthened beams. Figure-12 illustrates the typical rupture of GFRP with intermediate concrete (IC) debonding failure of strengthened beams in this series. The load-deflection behaviour for beams in the fourth series is shown in Figure-13. The curves represent a less ductile behaviour for beams FSB-C1 and FSB-C2 between steel yielding and failure as compared to that of the control beam CB. Beam FSB-C2 bonded with two layers of GFRP reinforcement slightly achieved better performance in flexural stiffness as compared to the beam FSB-C1. Upon further loading, the flexural cracks, in beams FSB-C1 and FSB-C2, were initiated between the constant bending moment region at a load of 42.1kN and 33.7kN, respectively. The beams FSB-C1 and FSB-C2 failed in rupture of GFRP with intermediate concrete (IC) debonding at a peak load of

137.15kN and 149.55kN with the corresponding maximum deflection values of 28.16 mm and 27.89 mm. From Figure-14 it is clear that the GFRP strengthened beams with additional GFRP closed end anchorages, sustained higher loads and achieved excellent performance regarding flexural capacity and stiffness than the GFRP strengthened beams without end anchorages. The experimental results are summarised in Table-4.

3.2 Ultimate Moment Capacity

The percentage increase in ultimate moment capacity of all the bi-directional GFRP strengthened beams over the control beam are presented in Table-5. The experimental results have shown that the externally strengthened RC beams with different end anchorages were effective in enhancing the flexural capacity by 36-68% over the control beam. From Figure-15, it is clear that the beam FSB-UA1 with one layer of GFRP reinforcement and U-GFRP strips end anchor achieved 44% increase in ultimate moment capacity, higher than the beam FSB-C1 that gave a moment capacity increase of 36% over the control beam CB. The U-GFRP strip anchor in beam FSB-UA1 was significant because the beam exhibited a 6% increase in ultimate moment capacity over beam FSC-C1 of the same level of flexural strengthening. However, beam FSB-CA2 with closed GFRP strip anchorage achieved 68% increase in ultimate moment capacity over the control beam, and it is higher than all the strengthened beams. By comparing the first (FSB-CA1 and FSB-CA2) and fourth (FSB-C1 and FSB-C2) series beams, it is clearly seen that the presence of closed GFRP strip end anchorage system in the first series beams significantly improved the flexural moment capacity of the beams by 6.7 and 13.8% over the beams FSB-C1 and FSB-C2, respectively. It is also clear from Figure-15 that beams FSB-SA1 and FSB-SA2 achieved an ultimate moment capacity increase of 4.7% and 4.9% over beams FSB-C1 and FSB-C2. This might be attributed to the metallic rigidity of the steel plate anchorage system in beam FSB-SA1 and FSB-SA2. The experimental results show that addition of end anchorages of steel plate or GFRP strips to RC beams strengthened in flexure enhanced the ultimate moment capacity of the beams. However, the moment capacity increase for the GFRP strengthened beams was observed to be within the strength increase of up to 40% as recommended by ACI 440 committee (2008).

3.3 Ductility

Ductility of RC beam can be defined as its ability to deform under loading prior to total collapse without loss in ultimate load carrying capacity (Spadea et al., 2015).

The ductility of the investigated GFRP strengthened beams decreased as compared to that of the control beam. Ductility is determined by considering the deflection or curvature of the beam. This study only focused on deflection ductility (μ_δ). The deflection ductility is defined as the ratio of ultimate deflection (δ_y) to yield deflection (δ_u) i.e.

$$\mu_\delta = \frac{\delta_u}{\delta_y} \quad (1)$$

Table-6 presents the calculated ductility index (μ_δ) and the ductility ratios of all the bi-directional GFRP strengthened beams to that of the control beam. These results confirmed that strengthening of RC beams with externally bonded bi-directional GFRP reinforcement resulted in significant loss in ductility of the strengthened beam. The deflection ductility ratio of all the strengthened beams was found to be 43%-54% of that of the original control beam. It is also observed that the ductility ratio of GFRP strengthened beams with anchorages, except the beam FSB-SA1, was relatively lower than that of GFRP strengthened beams without anchorages. The decrease in ductility was because the anchorage system at the ends controls the bond slip between the concrete and flexural GFRP reinforcement. Beam FSB-SA1 experienced the largest ductility index of 2.97. This indicates that the presence of steel anchorage has an insignificant effect on the ductility of the tested beams and result in only 2% increase in ductility index over beam FSB-C1. Figure-16 illustrates the ductility ratios of the bi-directional GFRP strengthened and the control beams.

4. THEORETICAL EVALUATION

According to with ACI Committee 440 Report, (2008), the ultimate moment resistance of RC beams strengthened with FRP reinforcement can be determined using strain compatibility method and equilibrium equation. Figure-18 shows the internal stress, and strain distribution of a singly reinforced concrete beam section strengthened in flexure with FRP. The ultimate moment resistance (M_u) of the section can be computed using Equation (2).

$$M_u = A_s f_s\left(d - \frac{\beta_1 c}{2}\right) + \psi_f A_f \varepsilon_{fd} E_f\left(h - \frac{\beta_1 c}{2}\right) + A'_s f'_s\left(\frac{\beta_1 c}{2} - d'\right) \quad (2)$$

where, A_f is the area of FRP reinforcement; A_s is the Cross-sectional area of tension steel reinforcement; A'_s is the Cross-sectional area of compression steel reinforcement c is the extreme distance from compression fibre to the neutral axis; d is the distance from extreme compression fibre to the centroid of tensile reinforcement; d' is the Depth of compression steel; E_f is the elastic modulus of FRP reinforcement; f_s is the stress in tensile reinforcement; f'_s is the stress in compression steel reinforcement; h is the overall depth of beam; $\beta_1$is the ratio of the depth of equivalent rectangular stress block to a depth of the neutral axis; ψ_f is the fibre reduction factor taken as 0.85 recommended by ACI Committee 440 Report, (2008) for flexural RC members with FRP external reinforcement to account for FRP uncertainties.

The ultimate theoretical moment of resistance (M_u) for all the bi-directional GFRP strengthened beams are computed using Equation (2) by considering the debonding strain (ε_{fd}) adopted by the relevant design guidelines.

4.1 ACI 440.2R-08 Design Guide

The ACI Committee 440 Report, (2008) proposed a design equation for predicting the debonding strain (ε_{fd}) to account for the premature IC debonding failure of the FRP plates. The debonding strain can be computed using the equation given below:

$$\varepsilon_{fd} = 0.41\sqrt{\frac{f'_c}{nE_{frp}t_{frp}}} \leq 0.9\varepsilon_{fu} \tag{3}$$

where, f'_c is the compressive strength of concrete; ε_{fu} is the rupture strain in FRP; t_{frp} is the thickness of FRP strip; and n is the number of FRP layers.

4.2 FIB Bulletin 14, (2001) Recommendations

The design guidelines of FIB Bulletin 14, (2001) give a design formula for predicting the total debonding strain base on fracture mechanics approach. The debonding strain is predicted as follows:

$$\varepsilon_{fd}=\alpha c_1 k_c k_b\sqrt{\frac{f_{ct}}{nE_f t_f}},\ \text{for}\ l_b \geq l_{b,max} \tag{4a}$$

$$\varepsilon_{fd}=\alpha c_1 k_c k_b\sqrt{\frac{f_{ct}}{nE_f t_f}}\frac{l_b}{l_{b,max}}\left(2-\frac{l_b}{l_{b,max}}\right),\qquad \text{for}\ l_b < l_{b,max} \tag{4b}$$

$$l_{b,max}=\sqrt{\frac{nE_f t_f}{c_2 f_{ct}}} \tag{4c}$$

$$k_b=1.06\sqrt{\frac{2-\frac{b_f}{b}}{1+\frac{b_f}{400}}} \geq 1 \tag{4d}$$

where, α= reduction factor approximately equal to 0.9, to account for the influence of inclined cracks on the bond strength ($\alpha = 1$ for beams with sufficient internal and external shear reinforcement and in slab); c_1 and c_2 can be obtained through calibrations with test results are assumed to be 0.64 and 2; k_c is a factor accounting for the state of compaction of concrete (k_c can generally be assumed to be equal to 1, however for FRP bonded to concrete faces with low compaction e.g. faces, not in contact with formwork during casting, $k_c = 0.64$); and k_b is a geometry factor and is given in Equation (4d); b_f is the width of FRP laminate, with $\frac{b_f}{b} \geq 0.33$.

4.3 Japan Society of Civil Engineers (JSCE) Design Guidelines

The JSCE, (1997) recommends a design equation for predicting the total debonding strain (ε_{fd}) of continuous FRP sheets by interfacial fracture energy. According to JSCE, the debonding strain can be calculated from Equation (5) below:

$$\varepsilon_{fd} = \sqrt{\frac{2G_f}{nE_f t_f}} \quad (5)$$

where, G_f is the interfacial fracture energy between FRP laminate and concrete and its value is assumed to be 0.5 N/mm.

5. COMPARISON OF EXPERIMENTAL AND THEORETICAL RESULTS

Table-7 presents the comparison of experimental and predicted results of three design guidelines for FRP strengthened beams. The results show that ACI Committee 440 Report, (2008) gave a mean ratio of experimental to the predicted ultimate moment capacities of 1.43 and a corresponding variation coefficient of 3.9%. The mean ratio of the experimental to predicted ultimate moment capacities of bi-directional GFRP strengthened beams using FIB Bulletin 14, (2001) and JSCE, (1997) were found to be 1.53 and 1.59 with a variance coefficient of 4.5% and 5.8% respectively. The comparison of results indicates no significant difference between the relevant design guidelines with regards to the predicted ultimate moment capacities of the bi-directional GFRP strengthened RC tested beams with and without end anchorages. However, the results indicate that ACI Committee 440 Report, (2008) design recommendation provides reasonably acceptable predictions for the ultimate moment capacities of the tested beams strengthened externally with bi-directional GFRP reinforcement followed FIB Bulletin 14, (2001) and eventually JSCE, (1997).

6. CONCLUSIONS

The experimental results of effects of anchorages (i.e. U-shaped, closed, and steel plate anchors) on reinforced concrete beam strengthened in flexure with the bi-directional glass fibre reinforced polymer (GFRP) were presented. A comparison was made between the experimental results and theoretical predictions based on ACI 440, (2008), JSCE (1997) and FIB Bulletin 14 (2001) design recommendations. The following findings can be summarised as follows:

1. The flexural bi-directional GFRP strengthening of reinforced concrete beams with different end anchorages (i.e. U-shaped, closed, and steel plate anchors) was found to be effective for enhancing the flexural effectiveness of the beams in terms of stiffness and ultimate moment capacity (36-68%).
2. The unanchored GFRP strengthened beams were failed in GFRP rupture with IC debonding failure whereas all the GFRP strengthened beams anchored at the GFRP plate ends failed in rupture of GFRP reinforcement with concrete crushing.
3. Experimental results confirm that the bi-directional GFRP strengthened beams with closed GFRP strip end anchors exhibited the highest performance in ultimate moment capacity of 45 - 68% of the control beam followed by two layers GFRP flexural strengthened beam with steel plate anchor archiving an ultimate capacity increase of 55%.

4. The ductility of all the strengthened beams with or without end anchorages was found to be 34%-54% of that of the original control beam. This evidently indicates that strengthening of RC beams with externally bonded bi-directional GFRP reinforcement and end anchorages resulted in significant loss of structural ductility of the strengthened beam.
5. The results of the comparison of experimental and theoretical predictions show that ACI Committee 440 (2008) design recommendation provides reasonably acceptable predictions for the ultimate moment capacities of the tested beams strengthened externally with bi-directional GFRP reinforcement followed by FIB Bulletin 14 (2001) and eventually JSCE (1997).

References

ACI Committee 318 (2008) *Building Code Requirements for Structural Concrete*. ACI 318-08. *American Concrete Institute*, Famington Hills, USA.

ACI Committee 440 Report (2008) *Guide for the Design and Construction of Externally Bonded FRP Systems for Strengthening Concrete Structures*. ACI 440.2R. Farmington Hills, USA.

Al-Amery R and Al-Mahaidi R (2006) "Coupled flexural-shear retrofitting of RC beams using CFRP straps". *Composite Structures* 75(1–4): 457–464.

Anania L, Badalà A and Failla G (2005) "Increasing the flexural performance of RC beams strengthened with CFRP materials". *Construction and Building Materials* 19(1): 55–61.

Aram MR, Czaderski C and Motavalli M (2008) "Debonding failure modes of flexural FRP-strengthened RC beams". *Composites Part B: Engineering* 39(5): 826–841.

Baggio D, Soudki K and Noël M (2014) "Strengthening of shear critical RC beams with various FRP systems". *Construction and Building Materials* 66: 634–644.

Bencardino F, Spadea G and Swamy RN (2002) "Strength and Ductility of Reinforced Concrete Beams Externally Reinforced with Carbon Fiber Fabric". *ACI Structural Journal* 99(2): 163–171.

Benjeddou O, Ouezdou M Ben and Bedday A (2007) "Damaged RC beams repaired by bonding of CFRP laminates". *Construction and Building Materials* 21(6): 1301–1310.

BS 1881 part 125 (1986) *Method of mixing and sampling fresh concrete in the laboratory British Standard Institution*. 389 Chiswick high road London.

BS EN 1992-1-1 (2004) *Eurocode 2: Design of concrete structures - Part 1-1 : General rules and rules for buildings*. *British Standards Institution*, Brussels.

Buyle-Bodin F and David E (2004) "Use of Carbon Fibre Textile to Control Premature Failure of Reinforced Concrete Beams Strengthened with Bonded CFRP Plates". *Journal of Industrial Textiles* 33(3): 145–157.

Carlos TB, Rodrigues JPC, de Lima RCA, and Dhima D. (2018) Experimental analysis on flexural behaviour of RC beams strengthened with CFRP laminates and under fire conditions. *Composite Structures*, Elsevier 189: 516–528.

Ceroni F (2010) Experimental performances of RC beams strengthened with FRP materials. *Construction and Building Materials*, Elsevier Ltd 24(9): 1547–1559.

Chahrour A and Soudki K (2005) Flexural Response of Reinforced Concrete Beams Strengthened with End-Anchored Partially Bonded Carbon Fiber-Reinforced Polymer Strips. *Journal of Composites for Construction* 9(2): 170–177.

Dat Duthinh and Monica Starnes (2001) Strengthening of Reinforced Concrete Beams with Carbon FRP. *Composites for Construction* 1: 493–498.

Fédération Internationale Du Béton (2001) *Externally bonded FRP reinforcement for RC structures. Bulletin*, Lausanne, Switzerland.

Fu B, Teng JG, Chen GM, Chen JF and Guo YC. (2018) Effect of load distribution on IC debonding in FRP-strengthened RC beams: Full-scale experiments. *Composite Structures*, Elsevier 188: 483–496.

G. Spadea, F. Bencardino and RNS (2000) Optimizing the performance characteristics of beams strengthened with bonded CFRP laminates Load. *Materials and Structures* 33(March): 119–126.

Gao B, Leung CKY and Kim JK (2005) Prediction of concrete cover separation failure for RC beams strengthened with CFRP strips. *Engineering Structures* 27(2): 177–189.

Grelle S V. and Sneed LH (2013) Review of Anchorage Systems for Externally Bonded FRP Laminates. *International Journal of Concrete Structures and Materials* 7(1): 17–33.

Hollaway, L.C. and Teng JG (2008) *Strengthening and Rehabilitation of civil infrastructures using Fibre-Reinforced Polymer (FRP) composites.* Elsevier.

Hollaway LC (2010) A review of the present and future utilisation of FRP composites in the civil infrastructure with reference to their important in-service properties. *Journal of Construction and Building Materials*, Elsevier Ltd 24(12): 2419–2445.

Hosen MA, Jumaat MZ, Alengaram UJ and Sulong NH. (2018) CFRP strips for enhancing flexural performance of RC beams by SNSM strengthening technique. *Construction and Building Materials*, Elsevier 165: 28–44.

J. G. Teng, J. F. Chen, S. T. Smith and L. Lam (2002) *FRP Strengthened RC Structures*. Wiley, John and Sons Ltd, West Sussex, England:

J.G. Teng JFC and STS (2001) Debonding Failures in FRP-Strengthened RC Beams: Failure Modes, Existing Research and Future Challenges 3. In: A reality Capri (ed.), *Proceeding of Workshop on Composites in Construction*, Italy, pp. 20–21.

Japan Society of Civil Engineers (JSCE) (1997) Recommendations for upgrading of concrete structures with use of continuous fiber sheets. In: Tokyo, p. 88.

Jayaprakash J, Abdul Samad AA, Koh HB, Anwar MP and Mohamad N. (2015) Experimental and Finite Element Studies Strengthened RC Rectangular Beams in Shear on CFF. *International Journal of Integrated Engineering* 7(1): 29–38.

Kalfat R and Smith ST (2013) Anchorage Devices Used to Improve the Performance of Reinforced Concrete Beams Retrofitted with FRP Composites : State-of-the-Art Review. *Journal of Composites for Construction* 17(February): 14–33.

Kim HS and Shin YS (2011) Flexural behavior of reinforced concrete (RC) beams retrofitted with hybrid fiber reinforced polymers (FRPs) under sustaining loads. *Composite Structures*, Elsevier Ltd 93(2): 802–811.

L. Lam and J.G. Teng (2001) "Srength of RC Cantilever Slabs Bonded with GFRP Strips". *Composites for Construction* 5(November): 221–227.

Leung CK and Yang Y (2006) "Energy-Based Modeling Approach for Debonding of FRP Plate from Concrete Substrate". *Journal of Engineering Mechanics* 132(6): 583–593.

Leung HY (2002) "Strengthening of RC beams: some experimental findings". *Structural Survey* 20(5): 173–181.

Li L, Guo Y and Liu F (2008) "Test analysis for FRC beams strengthened with externally bonded FRP sheets". *Construction and Building Materials* 22(3): 315–323.

Nurbaiah MN, Hanizah AH, Nursafarina A and Nur Ashikin M. (2010) "Flexural behaviour of RC beams strengthened with externally bonded (EB) FRP sheets or Near Surface Mounted (NSM) FRP rods method". *CSSR 2010 - 2010 International Conference on Science and Social Research* (Cssr): 1232–1237.

Pham HB and Al-Mahaidi R (2006) "Prediction Models for Debonding Failure Loads of Carbon Fiber Reinforced Polymer Retrofitted Reinforced Concrete Beams". *Journal of Composites for Construction* 10(February): 48–59.

Rafi MM, Nadjai A, Ali F and Talamona D. (2008) Aspects of behaviour of CFRP reinforced concrete beams in bending. *Construction and Building Materials* 22(3): 277–285.

Said H and Wu ZS (2008) "IC debonding in FRP-strengthened structures : experimental study". In: *Fourth International Conference on FRP Composites in Civil Engineering (CICE2008)*, Zurich, Switzerland, pp. 22–24.

Smith ST (2010) "Strengthening of Concrete, Metallic and Timber Construction Materials with FRP Composites". *The 5th International Conference on FRP Composites in Civil Engineering (CICE 2010)*: 13–19.

Smith ST and Teng JG (2003) "Shear-Bending Interaction in Debonding Failures of FRP-Plated RC Beams". *Advances in Structural Engineering* 6(3): 183–199.

Spadea, G., Bencardino, F. and Swamy RN (1998) "Structural behavior of composite RC beams with externally bonded CFRP". *Composites for Construction* 2, No. 3(3): 132–137.

Spadea G, Bencardino F, Sorrenti F, and Swamy RN. (2015) "Structural effectiveness of FRP materials in strengthening RC beams". *Engineering structures*, Elsevier Ltd 99: 631–641.

Sundarraja MC and Rajamohan S (2008) "Flexural Strengthening Effect on RC Beams by Bonded

Composite Fabrics". *Journal of Reinforced Plastics and Composites* 27(14): 1497–1513.

Teng JG and Chen JF (2007) "Debonding Failures of RC Beams Strengthened with Externally Bondded FRP Reinforcement : Behaviour and Modelling Classification of Failure Modes". In: *Asia-Pacific Conference Proceedings on FRP in Structures (APFIS 2007)*, Hongkong China, pp. 33–42.

Teng JG, Smith ST, Yao J and Chen JF. (2003) "Intermediate crack-induced debonding in RC beams and slabs. *Construction and Building Materials* 17(6–7): 447–462.

Toutanji H, Zhao L and Zhang Y (2006) "Flexural behavior of reinforced concrete beams externally strengthened with CFRP sheets bonded with an inorganic matrix". *Engineering Structures* 28(4): 557–566.

Triantafyllou GG, Rousakis TC and Karabinis AI (2017) "Corroded RC beams patch repaired and strengthened in flexure with fiber-reinforced polymer laminates". *Composites Part B: Engineering*, Elsevier 112: 125–136.

Wang J and Zhang C (2008) "Nonlinear fracture mechanics of flexural-shear crack induced debonding of FRP strengthened concrete beams". *International Journal of Solids and Structures* 45(10): 2916–2936.

Wu Y and Huang Y (2008) "Hybrid Bonding of FRP to Reinforced Concrete Structures". *Journal of Composites for Construction* 12(3): 266–273.

Yalim B, Kalayci AS and Mirmiran A (2008) "Performance of FRP-Strengthened RC Beams with Different Concrete Surface Profiles". *Journal of Composites for Construction* 12(6): 626–634.

Yang X, Gao W-Y, Dai J-G, Lu Z-D and Yu K-Q. (2018) "Flexural strengthening of RC beams with CFRP grid-reinforced ECC matrix". *Composite Structures*, Elsevier 189: 9–26.

Zhang HW and Smith ST (2012) "Influence of FRP anchor fan configuration and dowel angle on anchoring FRP plates". *Composites Part B: Engineering*, Elsevier Ltd 43(8): 3516–3527.

Table-1. Results of compressive and tensile strength of concrete

Specimen	Compressive Strength f'_c (N/mm^2)	Average Compressive strength of concrete $f'_{c,average}$ (N/mm^2)	Average tensile strength of concrete $f_{ct}=0.7\sqrt{f'_{c\ ave}}$ (N/mm^2)
CB	27.56	25.39	3.53
	24.55		
	29.75		
	19.71		
FSB-UA1 FSB-UA2 FSB-CA2	24.83	28.40	3.73
	32.97		
	32.51		
	23.29		
FSB-SA2 FSB-CA1	24.69	25.66	3.55
	23.61		
	23.99		
	30.36		
FSB-C1 FSB-C2 FSB-SA1	21.42	23.69	3.41
	20.48		
	21.42		
	31.45		

Where, f_{ct}= concrete tensile strength (ACI Committee 318, 2008)

Table-2. Properties of bi-directional GFRP fabric and epoxy resin as far manufacturer's manual

Materials	Properties	
GFRP (E-glass woven fabric)(EWR 600-100)	Tensile Strength (N/mm^2)	3850
	Modulus of elasticity (N/mm^2)	70000
	Rupture strain (mm/mm)	0.055
	Thickness (mm)	0.6
Epoxy Resin	Tensile strength (kg/cm^2)	800±50
	Flexural strength (kg/cm^2)	375±50

Table-3. Outline of the test beams

Series	Specimen Designation	Average Compressive strength of concrete	Number of GFRP layers	Types of Anchorage
-	CB	25.39	-	-
1st	FSB-CA1	25.66	1	GFRP closed-wrap
	FSB-CA2	28.40	2	
2nd	FSB-UA1	28.40	1	GFRP U-wrap
	FSB-UA2	28.40	2	
3rd	FSB-SA1	23.69	1	Fastened with steel plate and blot
	FSB-SA2	25.66	2	
4th	FSB-C1	23.69	1	-
	FSB-C2	23.69	2	-

Table-4. Summary of experimental test results

Specimen	Yield Load P_y (KN)	Mid-span deflection at yield load δ_y (mm)	Failure Load P_u (KN)	Mid-Span deflection at failure load δ_u (mm)	Percentage P_u increase over the control beam (%)	Ductility index $\mu_\delta = \frac{\delta_u}{\delta_y}$	Modes of Failure
CB	84.20	8.20	101.05	44.81	-	5.46	FF
FSB-CA1	115.70	9.56	146.40	24.50	45	2.56	R - CC
FSB-CA2	134.70	10.54	170.18	26.97	68	2.56	R - CC
FSB-UA1	117.90	9.46	145.45	26.44	44	2.79	R - CC
FSB-UA2	124.90	9.61	155.35	24.98	54	2.60	R - CC
FSB-SA1	112.05	9.06	143.55	26.92	42	2.97	R - CC
FSB-SA2	129.90	10.11	156.90	23.88	55	2.36	R - CC
FSB-C1	110.90	9.65	137.15	28.16	36	2.92	R-IC
FSB-C2	118.90	9.69	149.55	27.89	48	2.88	R-IC

where: FF-C= Flexural failure, R - CC= rupture of GFRP reinforcement with crushing of concrete, Y-IC= rupture of GFRP with IC debonding failure

Table-5. Ultimate moment capacities of GFRP strengthened and control beams

Specimen	Experimental ultimate moment capacity (M_u) (kNm)	Percentage increase over Control beam (%)	Percentage increase over FSB-C1 (%)	Percentage increase over FSB-C2 (%)
CB	20.21	-	-	-
FSB-CA1	29.28	45	6.7	
FSB-CA2	34.04	68	-	13.8
FSB-UA1	29.09	44	6.1	
FSB-UA2	31.07	54	-	3.9
FSB-SA1	28.71	42	4.7	
FSB-SA2	31.38	55	-	4.9
FSB-C1	27.43	36	-	-
FSB-C2	29.91	48	-	-

Table-6. Results of deflection, ductility index, and ductility ratio

Specimen	**Mid-span deflection at yield load δ_y (mm)**	**Mid-Span deflection at failure load δ_u (mm)**	**Ductility index $\mu_\delta = \frac{\delta_u}{\delta_y}$**	**Ductility ratio $\mu_\delta / \mu_{\delta control}$**
CB	8.20	44.81	5.46	1.00
FSB-CA1	9.56	24.50	2.56	0.47
FSB-CA2	10.54	26.97	2.56	0.47
FSB-UA1	9.46	26.44	2.79	0.51
FSB-UA2	9.61	24.98	2.60	0.48
FSB-SA1	9.06	26.92	2.97	0.54
FSB-SA2	10.11	23.88	2.36	0.43
FSB-C1	9.65	28.16	2.92	0.53
FSB-C2	9.69	27.89	2.88	0.53

Table-7. Comparison of experimental and theoretical predictions

Specimen	**$M_{u\ exp}$ (kNm)**	**ACI**		**JSCE**		**FIB**	
		$M_{u\ ACI}$ (kNm)	**$\frac{M_{u,exp}}{M_{u,ACI}}$**	**$M_{u\ JSCE}$ (kNm)**	**$\frac{M_{u,exp}}{M_{u,JSCE}}$**	**$M_{u\ FIB}$ (kNm)**	**$\frac{M_{u,exp}}{M_{u,FIB}}$**
FSB-C1	27.43	20.10	1.36	18.29	1.50	18.99	1.44
FSB-C2	29.91	21.55	1.39	19.05	1.57	20.02	1.49
FSB-CA1	29.28	20.24	1.45	18.32	1.60	19.10	1.53
FSB-CA2	34.04	21.92	1.55	19.14	1.78	20.31	1.68
FSB-UA1	29.09	20.68	1.41	18.36	1.58	19.22	1.51
FSB-UA2	31.07	21.92	1.42	20.96	1.48	20.31	1.53
FSB-SA1	28.71	20.10	1.43	18.29	1.57	18.99	1.51
FSB-SA2	31.38	21.83	1.44	19.10	1.64	20.15	1.56
Mean			1.43		1.59		1.53
Standard deviation			0.06		0.09		0.07
Variance Coefficient (%)			3.9		5.8		4.5

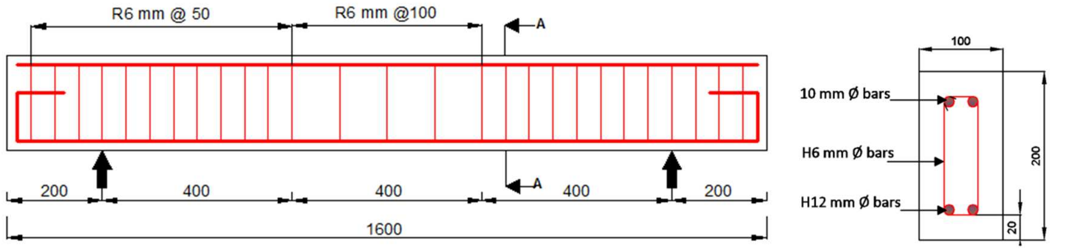

Figure-1. Reinforcement details of RC beams cross section A-A

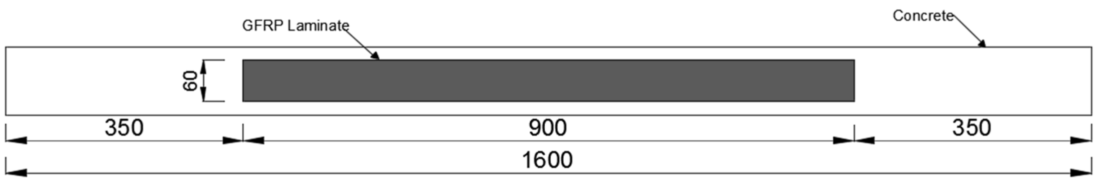

a. Soffit view of bi-directional GFRP strengthened beam specimen

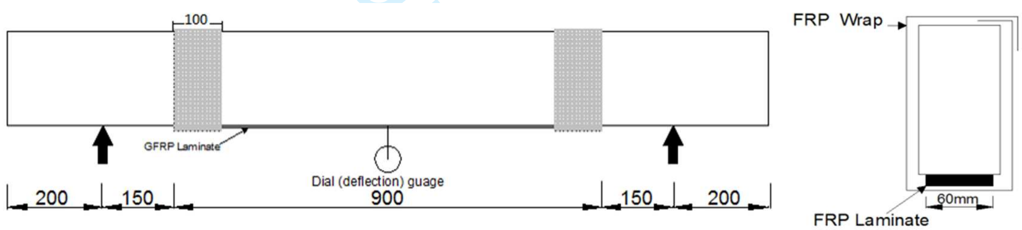

b. First Series beam specimen

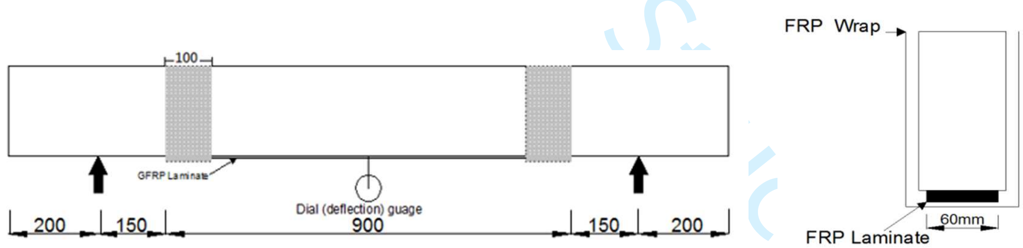

c. Second series beam specimen

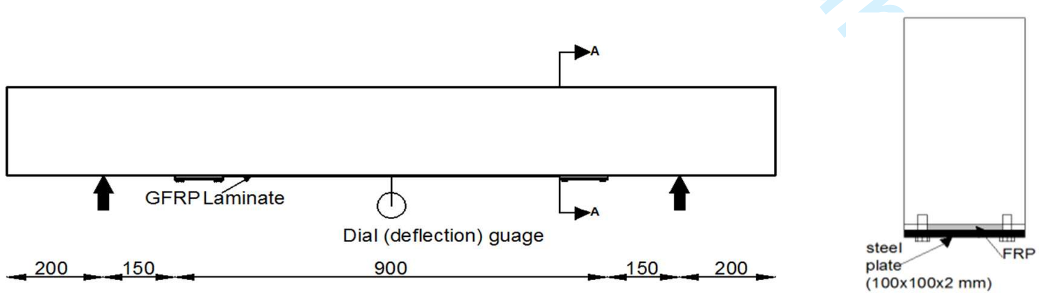

d. Third series beam specimen

Figure-2. Detail of beam strengthening scheme

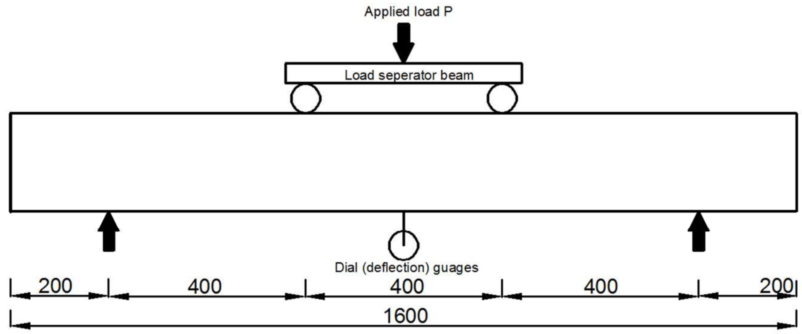

Figure-3. Experimental set-up of reinforced concrete beam

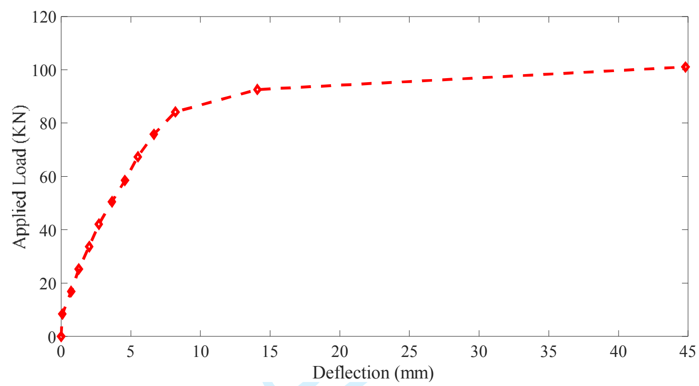

Figure-4. Load-deflection behaviour of control (CB) beam

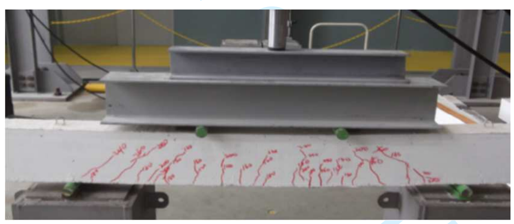

Figure-5. Flexural failure pattern of control beam (CB)

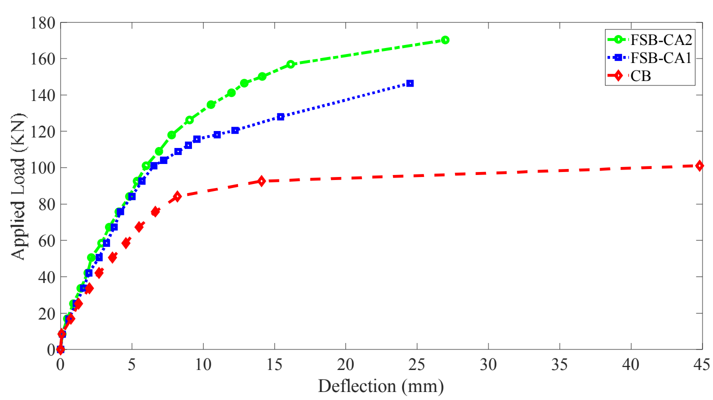

Figure-6. Load-deflection behaviour of FSB-CA1, FSB-CA2 and CB beams

(a) Rupture of GFRP with concrete crushing failure of beam FSB-CA1

(b) Rupture of GFRP with concrete crushing failure of beam FSB-CA2

Figure-7. Failure pattern of the first series beams with 1 and 2 layers of bi-directional GFRP reinforcement

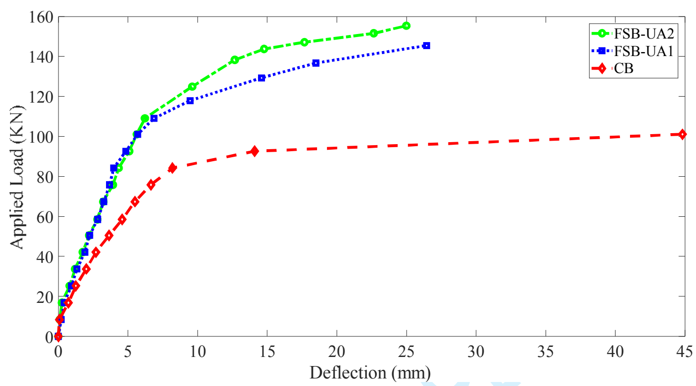

Figure 8. Load–deflection behaviour of FSB-UA1, FSB-UA2 and CB beams

(a) Rupture of GFRP with concrete crushing failure of beam FSB-UA1

(b) Rupture of GFRP with concrete crushing failure of beam FSB-UA2

Figure 9. Failure pattern of the second series beams with 1 and 2 layers of bi-directional GFRP reinforcement

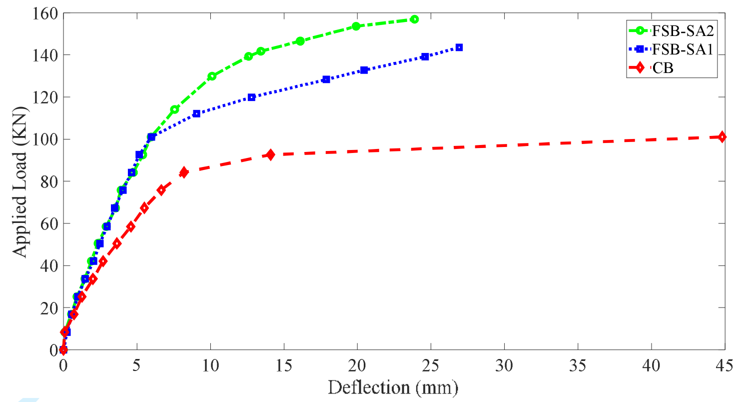

Figure 10: Load-deflection behaviour of beams FSB-SA1, FSB-SA2 and CB

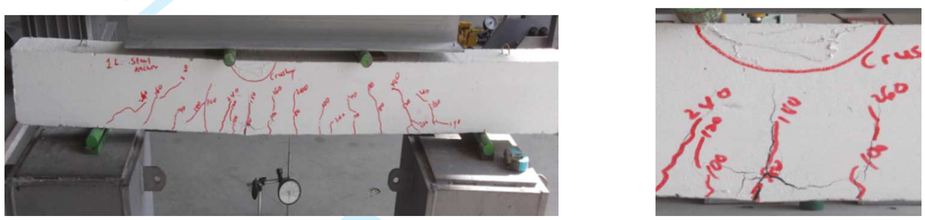

(a) Rupture of GFRP with concrete crushing failure of beam FSB-SA1

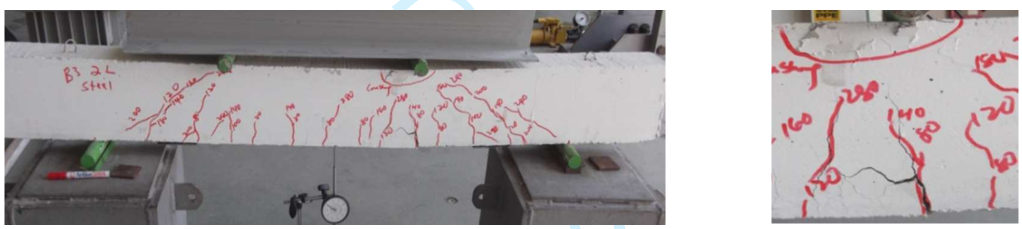

(b) Rupture of GFRP with concrete crushing failure of beam FSB-SA2

Figure-11. Failure pattern of the third series beams with 1 and 2 layers of bi-directional GFRP reinforcement

(a) Rupture of GFRP with intermediate concrete (IC) debonding failure of beam FSB-C1

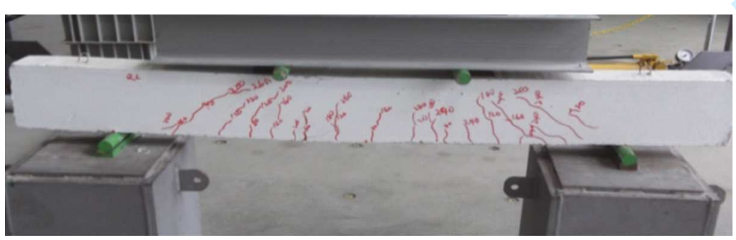

(b) Rupture of GFRP with intermediate concrete (IC) debonding failure of beam FSB-C2

Figure-12. Failure pattern of the fourth series beams with 1 and 2 layers of bi-directional GFRP reinforcement

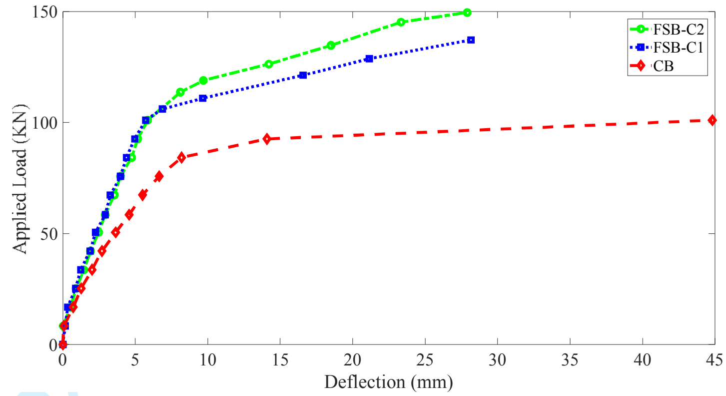

Figure-13. Load - Deflection behaviour of beams FSB-C1, FSB-C2 and CB

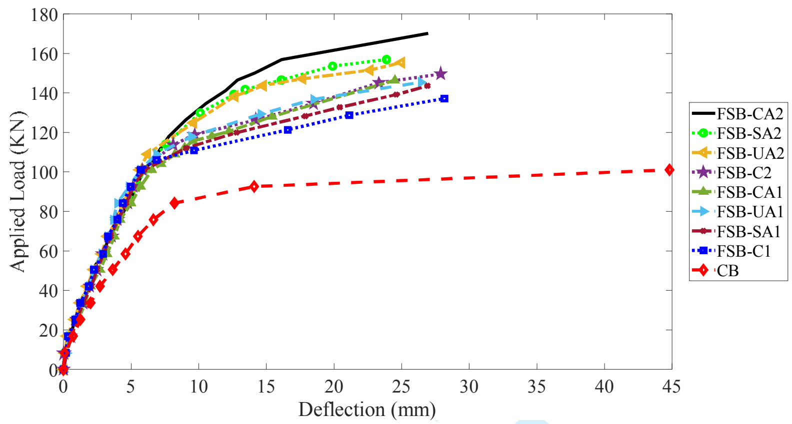

Figure-14. Load-deflection behaviour of all the strengthened beams and the Control beam

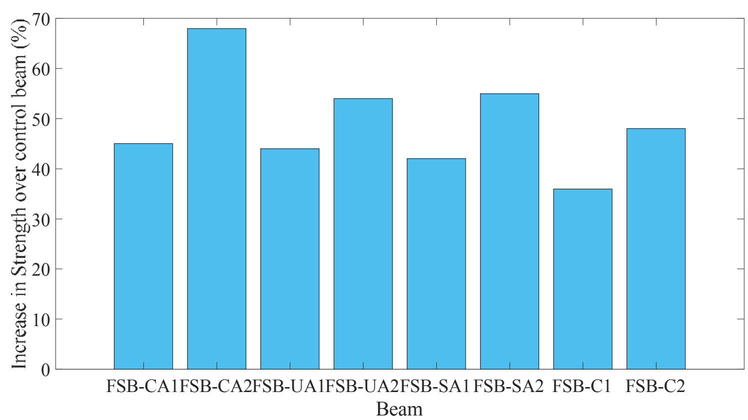

Figure-15. Ultimate moment capacity increase (%) over control beam

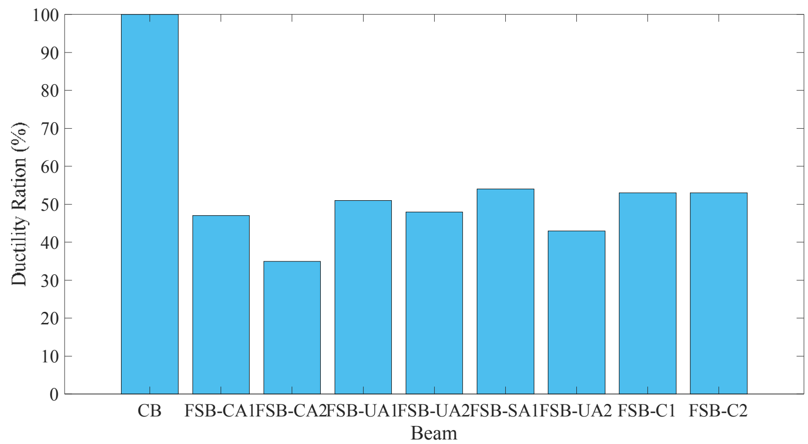

Figure-16. Ductility ratio of control and GFRP strengthened beams